

Thermal Numerical Analysis of PEM Fuel Cell Stack Using High Conductive Graphite Foam

Mnel A. H. Abdelgnei¹, Ali A. Hmad²

¹Department of Mechanical Engineering, Faculty of Materials Science and Engineering, Omar Al-Mukhtar University, El Beida, Libya.

²Department of Mechanical Engineering, University of Detroit Mercy, Detroit, USA

manal.elkalosh@omu.edu.ly, Hmadaa@udmercy.edu

Received 5 April 2023; revised 30 April 2023; accepted 30 April 2023

Abstract

This new study represents the use of graphite foam-type POCO for thermal management of proton exchange membrane fuel cells (PEMFC). The possibility of using airflow instead of a water flow cooling system was studied, and numerical analysis was conducted to investigate heat transfer improvement in graphite foam used in heat exchange applications. POCO foam was inserted between two heated plates and fluid air was forced to flow in the channel at different velocities. Both pressure drop across graphite foam and temperature distribution in flow direction were analyzed and will be discussed in this paper. The thermal local non-equilibrium was used to solve the energy equations. The high thermal conductivity of graphite foam makes it suitable for thermal management in PEMFC stack cooling applications. The temperature profile in x-direction on the heated plate was also investigated, and results showed an incredibly high-pressure drop through the applied graphite foam in the airflow direction, while the temperature was uniformly distributed across the heated plates. The result shows that graphite foam can be used in fuel cell thermal management.

Keywords—Graphite foam; PEMFC; POCO foam; Pressure drop; Temperature distribution.

1. Introduction

The magnificent physical properties of graphite foam, such as appropriate thermal conductivity and low density, make researchers interested in developing materials used for thermal management applications [1]. Some studies have extensively focused on the thermal properties of metal foam. Moreover, several researchers have studied heat transfer and pressure drop for a variety of metal foams, but few have studied heat transfer and pressure drop across graphite foam, specifically [2]. The application of metal foam has been studied in past years, especially in convective fluid flow heat transfer [3].

Metal foam is usually made of materials such as aluminum, copper, or carbon that have open cell structure and are produced either by foaming or casting. Those open voids allow the fluid to pass through to the internal surfaces in the forced flow. In general, graphite foam is made of carbonized foam and graphitized carbon [4]. Graphite material has a high conductivity compared to aluminum. Thus, it makes the graphite foam absorb heat and maintain heat transfer by forced convection. The advantages, such as high conductivity and high internal surface area of graphite foam, make it a good choice to use in heat transfer applications [5]. Hmad and Dukhan [6] presented a 2D simulation of the

PEM stack and studied the heat transfer enhancement in an air-cooled channel filled with metal foam. The results showed that the LTNE was a great assumption to solve the thermal equation and approved that metal foam was also a terrific candidate material for fuel cell thermal management.

A study done by Gallego and Klett [7] studied pressure drop and heat transfer in graphite foam by providing the first data on such an application.

Nomenclature	
C_p	Fluid heat capacity
h	Half-height of the channel
k	Thermal conductivity
K	Permeability
p	Pressure
q_{in}	Heat flux
T	Temperature
u	Fluid velocity
x	Coordinate in the flow direction
y	Coordinate normal to the wall
ρ	Fluid density
ϵ	Porosity

The study was only on the effect of pressure drop and heat transfer on graphite foam, but lacked details on the effects of some parameters, such as porosity, pore diameter, and Reynolds number, to investigate heat transfer. Another study published by Yu et al. [8] used the experimental work data to study convective heat transfer and pressure drop across graphite foam when the fluid forced to flow through the graphite foam. The same data were used to modify numerical models to study the differences between graphite foam and aluminum foam.

Additionally, Alam and Maruyama [9] experimentally proposed that graphite foam has wide-ranging thermal conductivities due to manufacturing process differences regarding heat treatments. Along the same lines, a study by Yu et al. [10] showed two models of graphite foam, the thermal model, and the hydrodynamic model, based on the foam's cubic cell unit. The results showed great agreement with the experimental data provided by Klett et al [11]. The thermal conductivity of graphite foam is six times greater than aluminum foam, which makes graphite foam a major candidate for heat exchanging applications [12].

Quite a few studies have investigated the effects of airflow on heat transfer in graphite foam [13]. Using graphite foam as a heat sink in applications such as energy storage systems has been considered [14]. The behavior of the panel sandwich of graphite foam has been studied and published in some academic publications [15]. A study published by Gallego et al. [16] proved that using graphite foam as a heat sink reduces the size of the air-cooled system and eliminates the water-cooled system as well. Thermally, graphite foam is greater than aluminum foam; a heat sink made of graphite foam transfers heat faster than a heat sink made of aluminum. Williams et al. [17] made a comparison between two heat exchangers: one used fins made of copper and the other used graphite foam. The heat exchanger that uses graphite foam has a significant ability to exchange heat.

This research study proposes the possible use of graphite foam type POCO for heat transfer enhancement on the PEMFC. The researcher inserted graphite foam into micro-air channels of the PEMFC as a heat exchanger, using forced air as a coolant instead of water flow, thereby eliminating cooling system accessories. It was found that the energy equation can be solved with the thermal local non-equilibrium. The numerical analysis investigates pressure drop and heat transfer improvement in graphite foam. The distribution of temperature across the plate length will also be discussed.

2. Numerical analysis

Numerical analysis on graphite type POCO micro-channel was investigated, along with heat transfer and pressure drop. The temperature profile in flow direction at various velocities and the effects of graphite foam on heat transfer were studied. Table 1 shows applied POCO foam properties including density, porosity, pore diameter, permeability, and surface area density.

Table.1 Graphite foam thermal parameters

Material	Pore diameter	Density	Thermal conductivity	Permeability	Surface area density
HTC POCO	500 (μm)	0.55 (g/cm ³)	135 (W/m.k)	6.13E- 03(m ²)	5240 (m ² /m ³)

2.1. Governing equations:

The 2D of (x-y) coordinates of a microchannel filled with graphite foams is illustrated in Fig.1. The airflow was assumed to be steady, incompressible through the channel, and in thermal equilibrium state.

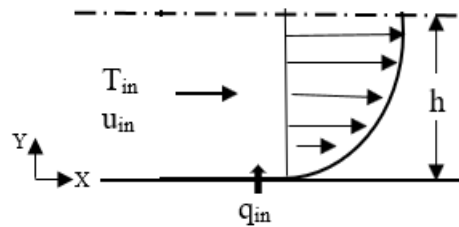


Fig.1 A 2D coordinate system of an air channel.

The fully developed flow region was in Darcian model behavior. The Darcy and energy equations are given by Eq. 1 and 2,

$$\frac{\mu}{\varepsilon} \frac{d^2 u}{dy^2} - \frac{\mu}{K} u = \frac{dP}{dx} \quad (1)$$

$$\rho C_p u \frac{\partial T}{\partial x} = k \frac{\partial^2 T}{\partial y^2} \quad (2)$$

where u is the velocity in the flow direction, T is the temperature, q_{in} is the constant heat flux applied on both walls, μ is fluid viscosity, while ε is the porosity, and K is the permeability of the graphite foam, respectively. The viscous effects in the first part of Eq.(1) are expressed in the Brinkman term ($\frac{\mu}{\varepsilon} \frac{d^2 u}{dy^2}$), whereas the second part of the equation ($-\frac{\mu}{K} u = \frac{dP}{dx}$) denoted the Darcian model.

2.2. Boundary conditions:

Only the lower half of the channel was considered since it is symmetrical across the centerline. Eqs. (3) and (4) show the applicable boundary conditions for half of the applied air channel.

$$y = 0: \quad \frac{du}{dy} = 0, \quad \frac{\partial T}{\partial y} = 0 \quad (3)$$

$$y = h: \quad u = 0, \quad \frac{\partial T}{\partial y} = \frac{q_{in}}{k} \quad (4)$$

3. Results and discussion

3.1. Pressure drop in the x-direction

The pressure drop in x-direction through graphite foam is illustrated in Fig.2. Pressure drop in flow direction across the graphite foam type POCO sample at different inlet flow velocities ranged from 0.2 to 0.7 m/s, as illustrated in Fig.2. It was observed that the pressure drop in graphite foam increases with the increase of the inlet velocity. This increase in velocity is directly proportional to the increase in pressure drop, which is depicted in Eq.1.

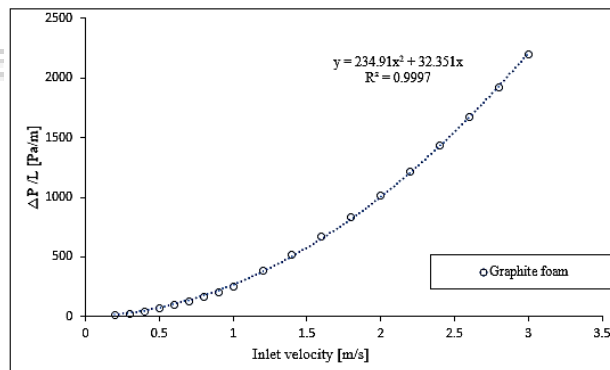


Fig.2 Pressure drop for graphite foam at a different inlet velocity.

3.2. Airflow temperature in the y-direction

The comparison between airflow temperatures in y-direction was investigated and is shown clearly in Fig.3, which shows the difference in the air temperatures with different airflow velocities. It was observed that more heat was absorbed by graphite foam. The air temperature near the heated plate was approximately equal to the plate temperature, which was the highest air temperature in the whole design. It is important to note that increasing the inlet velocity dropped the air temperature to a

certain temperature at a higher position until reaching the lowest temperature in the center of the airflow. The temperature was uniformly distributed across the air channel. The same behavior was seen at the centerline of the air channel, where the fluid temperature decreased with the increase of inlet air velocity.

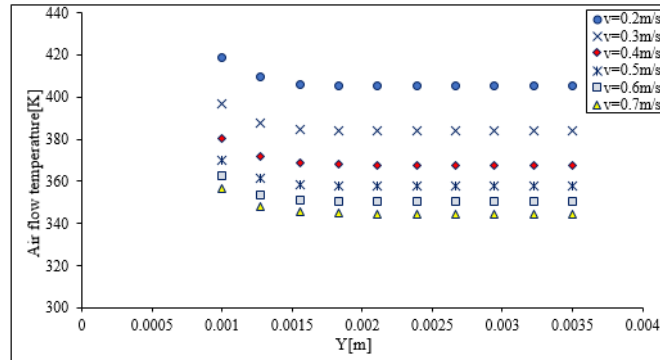


Fig.3 Airflow temperature in y-direction at different air velocities

3.3. Plate temperature in the x-direction

Figure 4 shows the plate temperature distribution at different inlet air velocities from 0.2 to 0.7 m/s in the x-direction. It was observed that increasing the airflow velocity decreased plate temperature. When inlet velocity was 0.2 m/s, the plate temperature in x-direction was far from safe range temperature. However, increasing airflow velocity affected the plate temperature, and the plate temperature reached the safe range at an inlet velocity of 0.6m/s. This decrease in temperature was sustained with the increase of airflow velocity.

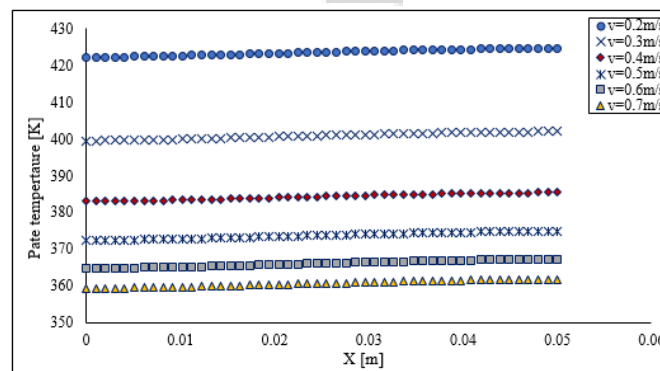


Fig.4 Plate temperature in the x-direction at different air velocities

3.4. Maximum plate temperature

The comparison between maximum airflow and plate temperatures at different inlet flow velocities is illustrated in Fig.5. Both airflow temperature and plate temperature were high at the inlet where the inlet velocity was 0.2m/s. The airflow temperature through the foam was 10 degrees lower than the plate temperature. Increasing airflow velocity reduces both maximum temperatures until reaching the

lowest temperature at 3m/s. The temperature's uniform distribution behavior was seen at the centerline of the air channel and the centerline of the heated plate with the increase of velocity.

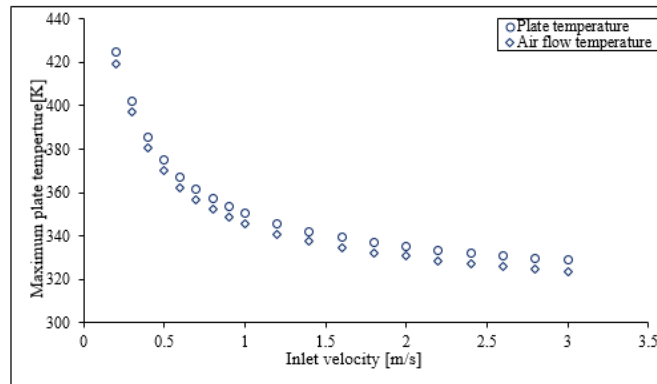


Fig.5 Maximum temperatures at different inlet velocities

3.5. Maximum plate temperature contours

Regarding temperature distribution, the contours are seen in Fig.6. The figure shows a 5-degree difference between plate and air temperature distributions. In the plate temperature distribution contour, the difference between both contours was observed. Increasing the air inlet velocity had a substantial effect on cooling plate temperatures. The maximum plate temperature was 424K at 0.2 m/s air velocity, higher than temperatures at other inlet velocities, as illustrated in Fig. 6-a. Depicted in Fig.6-b), the maximum temperature was 20 degrees lower than the first plate temperature at 0.2 m/s inlet velocity. The effect of increasing inlet velocity is displayed in Fig.6-c) where the maximum temperature was lower than the previous readings; thus, increasing the inlet velocity from 0.3 m/s to 0.4 m/s decreased the plate temperature to 374K, shown in Fig.6-d.

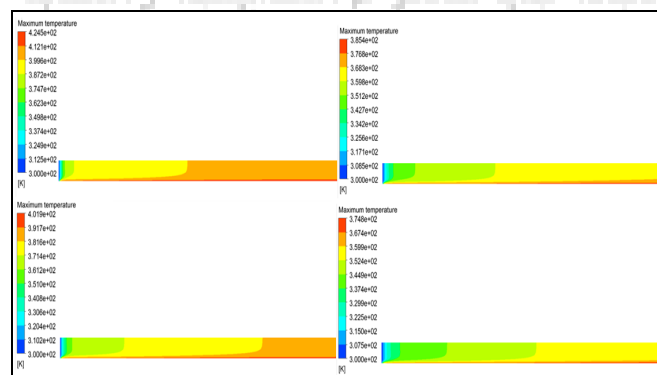


Fig.6 temperature contours a) at inlet velocity 0.2 m/s, b) at inlet velocity 0.3m/s, c) at inlet velocity 0.4m/s, d) at inlet velocity 0.5 m/s

4. Conclusion

The possibility of using graphite foam type POCO for thermal management of proton exchange membrane fuel cells was analytically studied and discussed in this paper. The pressure drop across graphite foam and temperature distribution in flow direction were also presented. The results showed an incredible drop in pressure across the graphite foam in the x-direction, and the temperature was uniformly distributed through the air channel and heated plates. It is important to note that the temperature's uniform distribution behavior was seen at the centerline of the air channel in the y-direction with the increase in inlet flow velocity. The same behavior was seen at the centerline of the plate center line in the x-direction, where the fluid temperature decreased with the increase in inlet air velocity. Therefore, graphite foam type POCO foam has a thermal conductivity 10 times higher than aluminum foam, which makes graphite foam a reasonable applicant for thermal management of PEMFC stacks.

5. References

- [1] A.F. Abuserwal, E.M.E. Luna, R. Goodall, R. Woolley, the effective thermal conductivity of open cell replicated aluminium metal sponges, *Int. J. Heat Mass Transf.* 108(2017) 1439–1448.
- [2] G. Zaragoza, R. Goodall, Development of a device for the measurement of thermal and fluid flow properties of heat exchanger materials, *Int. J. Heat Mass Transf.* 56(2014) 37–49.
- [3] Hmad, Ali A., and Nihad Dukhan. 2021. "Cooling Design for PEM Fuel-Cell Stacks Employing Air and Metal Foam: Simulation and Experiment" *Energies* 14, no. 9: 2687.
- [4] Klett, W. J., Hardy, R., Romine, E., Walls, C., and Burchell, T., 2000, "High-Thermal Conductivity, Mesophase-Pitch-Derived Carbon Foam: Effect of Pre-cursor on Structure and Properties," *Carbon*,38, pp. 953–973.
- [5] Gallego, C. N., and Klett, W. J., 2003, "Carbon Foams for Thermal Management," *Carbon*,41, pp. 1461–1466.
- [6] Hmad A.A., Dukhan N. (2020) Cooling of PEM Fuel Cell Stacks Using Open-Cell Metal Foam. In: Dukhan N. (eds) *Proceedings of the 11th International Conference on Porous Metals and Metallic Foams (MetFoam 2019)*. The Minerals, Metals & Materials Series. Springer, Cham
- [7] Paek, W. J., Kang, H. B., Kim, Y. S., and Hyum, M. J., 2000, "Effective Thermal Conductivity and Permeability of Aluminum Foam Materials," *Int. J. Thermophys.*,212, pp. 453–464.

- [8] Yu, Q., Thompson, B. E., and Straatman, A. G., 2006, "A Unit-Cube Based Model for Heat Transfer and Pressure Drop in Porous Carbon Foam," ASMEJ. Heat Transfer,128, pp. 352–360.
- [9] J.W. Klett, A.D. McMillan, N.C. Gallego, C.A. Walls, The role of structure on the thermal properties of graphite foams, J. Mater. Sci. 39 (2004) 3659–3676.
- [10] M.K. Alam, B. Maruyama, Thermal conductivity of graphitic carbon foams, Exp.Heat Transfer 17 (2004) 227–241.
- [11] Q.J. Yu, B.E. Thompson, A.G. Straatman, A unit cube-based model for heat transfer and fluid flow in porous carbon foam, ASME J. Heat Transfer 128(2006) 352–360.
- [12] W. Lin, J. Yuan, B. Sundén, Review on graphite foam as thermal material for heat exchangers, World Renewable Energy Congress, Sweden 2011, pp. 749–755.
- [13] M. Collins, Parametric Study of Graphite Foam Fins and Application in Heat Exchangers MS Thesis Florida State University, 2013.
- [14] P.G. Stansberry, E. Pancost, Evaluation of graphitic foam in thermal energy storage applications, in: W.M. Kriven, et al., (Eds.), Developments in Strategic Materials and Computational Design IV, American Ceramic Society (Wiley) 2014, pp. 151–155.
- [15] S. Mukundan, Structural Design and Analysis of a Lightweight Composite Sandwich Space Radiator Panel MS Thesis Texas A&M University, 2003.
- [16] N. C. Gallego, and J. W. Klett, Carbon foams for thermal management, Carbon 41, 2003, pp. 1461-1466.
- [17] Z. A. Williams, and J. A. Roux, Graphite foam thermal management of a high packing density array of power amplifiers, Journal of Electronic Packaging 128, 2006, pp. 456-465.